

# **Accelerated Curing and Drying Characteristics of a Porous Concrete Material by a Microwave-Dryer Prototype**

**N. Makul,<sup>a</sup> P. Rattanadecho<sup>b</sup>**

<sup>a</sup> *Department of Building Technology, Faculty of Industrial Technology, Phranakhon Rajabhat University, Changwattana Road, Bangkok, Bangkok 10220, Thailand.*

<sup>b</sup> *Center of Excellence in Electromagnetic Energy Utilization in Engineering (CEEE), Thammasat University (Rangsit Campus), Khlong Luang, Prathum Thani, 12121, Thailand.*

---

*Correspondence: P. Rattanadecho, Center of Excellence in Electromagnetic Energy Utilization in Engineering (CEEE), Thammasat University (Rangsit Campus), 99 Moo 18, Klong 1, Khlong Luang, Pathumthani 12120, Thailand  
E-mail: ratphadu@engr.tu.ac.th*

**ABSTRACT**

This article presents a way to use microwave-assisted drying to accelerate the curing of a porous concrete material. The design of a microwave dryer prototype is described together with experimental investigations into the drying characteristics of porous concrete subjected to the microwave drying process. Mathematical models were applied to design a horn-shaped microwave cavity and as a basis for constructing a stationary and a moving microwave dryer prototype that uses microwave energy at an operating frequency of 2.45 GHz and a power of 800 W. The experiments included the effects of microwave curing on the concrete's properties comprising temperature evolution, moisture content variation, and compressive strength development. Also, the porous concrete material was compared to water- and air-cured concretes on the basis of these properties. Based on the concept of antenna, a rectangular horn cavity of 246.7 mm × 333.68 mm is designed showing a uniform thermal distribution and conforming to the acceptance criterion of a suitable temperature of concrete curing. From the experiments, it was found that the application period for curing using the microwave-dryer prototype was considerably shorter than for conventional curing methods. The appropriate preheating interval is 30 min, and microwave energizing for 15 min/time and a paused duration of 60 min produces maximum compressive strength. However, the time needed for curing is considerable. When concrete is dried using microwave energy for more than 90 min at over 80 °C, the effect is a continuous decrease in compressive strength. Further, the compressive strength development of porous concrete subjected to microwave curing at early age is also greater than that achieved by curing via water soaking or air drying.

**Keywords:** Porous concrete; Accelerated Curing; Drying characteristic; Microwave energy; Prototype

## INTRODUCTION

Microwave-assisted drying (MD) has emerged as a popular kind of innovative drying technology resulting from microwave heating via liquid vaporization. A particularly efficient technique for thermal processes, MD can considerably reduce the time needed for drying, thereby saving energy. It is, therefore, widely used in various industrial processes including some relating to biological tissue,<sup>[1]</sup> wood,<sup>[2,3]</sup> food,<sup>[4-6]</sup> ceramics, and oil,<sup>[7,8]</sup>—as well as for the accelerated curing and repair of concrete<sup>[9-11]</sup>.

Up to the present time, the focus of research and development pertaining to the technology used to repair concrete has focused on saving the time taken to execute repairs. However, the time needed to cure concrete is still lengthy and the process relies on conventional curing technology for repairs such as applying a curing compound, water ponding,<sup>[12]</sup> and using a wetting sag to cover the concrete surface so that the moisture content of the concrete is retained. This long period leads to traffic jams because traffic lanes must be closed so that roads can be repaired. Therefore, any method such as the use of streams or hot air with the potential to reduce the time needed in the initial concrete-curing phase is of great interest. However, these methods have the drawback of producing intermittent thermal distribution in concrete, leading to a reduction in compressive strength and causing the internal structure to break down.<sup>[13]</sup> Therefore, microwave-drying technology applied to concrete curing in the initial phase is advantageous because heat can be produced in a way that is more efficient than with other methods.

It is well known that thermal-curing methods have an adverse effect on the properties of concrete—both at early age and in the long term. Therefore, a crucial question arises: Can the microwave-heating method be applied in the concrete industry? Theoretically, it is possible. This is because materials used to make concrete, such as hydraulic Portland cement, aggregates, water, and admixtures are dielectric; i.e., they can absorb microwave energy

effectively.<sup>[14-16]</sup> Water, in particular, has a relative dielectric constant ( $\epsilon_r'$ ) and loss tangent ( $\tan \delta$ ) with higher values than the other components of the concrete. As a result, when the electric field ( $\vec{E}$ ), which is a main part of the electromagnetic field, interacts with the concrete's constituents, microwave electromagnetic energy is quite dramatically transferred and then converted into heat via an interaction with water molecules. This mechanism causes the bonds to vibrate such that energy is dissipated as heat and transferred within the concrete to be processed thus giving rise to accelerated hydration reactions. Consequently, free water molecules in the capillary pores of the concrete are quickly removed from the internal concrete structure before setting, which means that plastic shrinkage from drying is taking place. The result is the collapse of the capillary pores and the simultaneous densification of the microstructure.

However, microwave-assisted drying is still limited in terms of the type of material to which it can be applied.<sup>[18,19]</sup> The disadvantage of this material is that its thermal distribution is inconsistent, which leads to problems associated with hot spots and cold zones.<sup>[20,21]</sup> Therefore, microwave distribution with multi-mode capability has been developed: There are microwave technology applications whereby concrete is heated such that its moisture content evaporates while heat is transferred to its top surface.

The present research focuses on the design and construction of a portable prototype for concrete curing that relies on applying microwave energy. Experiments are performed, and the results are reported. The studied parameters are temperature evolution, moisture content, curing time, compressive strength. Further, a comparison of microwave curing and conventional curing is also presented.

## **DESIGN OF A HORN-SHAPED CAVITY USING A MATHEMATICAL MODEL**

As shown in Fig. 1, the design processes focus on the study of a horn-shaped cavity and a mathematical model to analyze and determine the horn size, configuration, and cavity. A 3D mathematic model is considered via a finite element method, which is analyzed with COMSOL™ Multiphysics.<sup>[22]</sup> After that, the microwave-curing prototype is constructed. The horn of this prototype can be adjusted vertically. Microwave power of 800 W at 2.45 GHz is applied for the experiment, and fixed and movement modes are studied.

[Insert Fig. 1]

### **Mathematical formulation**

From the calculated horn size, the mathematical model is applied to determine the design size of the horn and to analyze the distribution of the magnetic field in the cavity (without load case) and the distribution of the concrete's temperature (load case). In this study, COMSOL™ Multiphysics<sup>[22]</sup> is conducted to create the mathematical model, which begins by calculating the horn size. Then, the mathematical model is applied to analyze and determine the optimal horn size before the horn is built.

The mathematical model analysis is divided into two parts, which are a distribution analysis of the magnetic field in the cavity and an analysis of the thermal distribution of the concrete. The physical model is presented in Fig. 2 with an input microwave position can be described in detail as follows:

1. The cavity constitutes the perfect conducting wall. Thus, the output of microwave energy from the waveguide is not absorbed.
2. The load is the material that can be heated by microwave energy. The load can absorb microwave energy and transform it into heat.
3. The waveguide functions as a source of microwave heat (the wave mode is  $TE_{10}$ ).

[Insert Fig. 2]

### Analysis of the magnetic field in the cavity

#### *A case without load*

The distribution of the magnetic field in the cavity (in terms of the guided wave, the cavity, and the load) can be found by using Maxwell's magnetic field equation [23], as in the case 3. This can be carried out by using the COMSOL<sup>TM</sup> Multiphysics program, the equation associated with which is as follows:

$$\nabla \times (\mu_r^{-1} \nabla \times E) - k_0^2 \left( \epsilon_r - \frac{j\sigma}{\omega\epsilon_0} \right) E = 0 \quad (1)$$

$$\epsilon_0 = n^2 \quad (2)$$

where  $E$  is the electric field intensity (V/m),  $H$  is the magnetic field intensity (A/m),  $J$  is the current density (A/m<sup>2</sup>),  $\sigma$  is the electric conductivity (S/m),  $\mu_r$  is the relative magnetic permeability,  $\omega$  is the angular velocity (rad/s),  $k_0$  is the free space wave number,  $\epsilon_0$  is the permittivity of the vacuum ( $8.85419 \times 10^{-12}$  F/m),  $n$  is the refractive index, and  $\epsilon_r$  is the relative dielectric constant that expresses the properties of the material in terms of its absorption capacity to transmit and reflect microwave energy.

The scope of the microwave distribution in the waveguide and the cavity constitutes the perfect conducting wall. Therefore, the scope of the cavity wall can be expressed as in this equation:

$$n \times E = 0 \quad (3)$$

The continuous scope of the microwave energy at the boundary between the load and the air in the cavity can be expressed as in this equation:

$$n \times (\nabla \times E) - jkn \times (E \times n) = -n (E_0 \times Jk(n-k)) (\exp(-Jk \cdot r)) \quad (4)$$

The magnetic field condition created by the wave guild, a microwave source, presented in Fig. 2, can be expressed as in this equation:

$$port : S = \int (E - E_1) \cdot E_1 / \int E_1 \cdot E_1, \quad (5)$$

where the port is the microwave source at a power of 800 W.

The initial condition of the magnetic field is defined as

$$E_x(t_0), E_y(t_0), E_z(t_0) = 0 \quad (6)$$

### ***A case with load***

The thermal transmission equation in this study is designed to analyze only the thermal distribution within load under the magnetic field in the cavity for the 3D case. On the assumption that the air in the cavity cannot absorb the microwave energy and transform it into heat, the internal load can transfer heat by conduction and the load can generate internal heat by transforming the microwave energy into heat. On this assumption, the heat-exchange equation can be written based on the background from the COMSOL<sup>TM</sup> Multiphysics program<sup>[22]</sup> as in this equation:

$$\rho C_p \frac{\partial T}{\partial t} + \nabla \cdot (-k \nabla T) = Q \quad (7)$$

where  $T$  is the temperature ( $^{\circ}\text{C}$ ),  $t$  is time (s),  $C_p$  is the heat capacity at constant pressure (J/kg.K),  $\rho$  is the density ( $\text{kg/m}^3$ ),  $k$  is the thermal conductivity (W/m.K), and  $Q$  is the local volumetric heat-generation term generated by the absorption of the microwave energy transmitted as heat ( $\text{W/M}^3$ ).

Heat can only be generated by the load or the concrete; therefore, the considered domain in terms of heat focuses directly on load. Thus, the boundary condition of heat occurs only on the top surface of the load (the wall of the load is an insulator that is cannot transmit heat).

The boundary condition of the heat surface at the top of the load is

$$n \cdot (-k \nabla T) = 0. \quad (8)$$

The boundary condition of the heat wall is

$$-n \cdot (-k \nabla T) = 0. \quad (9)$$

The initial condition of the heat analysis is

$$T(t_0) = 298.15 \text{ K} \quad (10)$$

### **Analysis of the horn size**



The analysis of the horn size is divided into two parts: an analysis of the distribution of the magnetic field within the cavity (without load) and an analysis of the thermal distribution of the concrete (with load). Time does not affect the magnetic field behavior within the cavity in this analysis, but time does affect the distribution of the magnetic field within the cavity. Thus, this is a steady-state problem. Therefore, the analysis of the distribution of the magnetic field within the cavity in 3D is carried out using the COMSOL™ Multiphysics program.<sup>[22]</sup>

In the analysis of the thermal distribution in the concrete, it was found that time had a direct effect on the temperature of the load. This problem is identified as a transient condition. Therefore, the analysis of the distribution of the concrete temperature is performed with the finite element method using the COMSOL™ Multiphysics program.<sup>[22]</sup>

The input data used to analyze both the magnetic field and the heat transfer are presented in [Table 1](#).

[\[Insert Table 1\]](#)

### Results of the model simulation

The modeling results of the magnetic field within the cavity in the shape of a horn (without load case) [\(Fig. 3a\)](#) and the thermal distribution in the concrete (with load case) are presented in [Fig. 3\(b\)](#).

In Case 1, the electric fields are  $8.25e^4 \times 10^4$  V/m,  $1.03e^5 \times 10^5$  V/m,  $1.068e^5 \times 10^5$  V/m, and  $8.74e^4 \times 10^4$  V/m, as presented in [Fig. 4](#). The electric fields are similar whereas the increased distribution of the electric field by an increase in the height of the horn [from ???](#) to 273 mm provides a progressive electric distribution of  $8.74e^4 \times 10^4$  V/m, as presented in [Fig. 4\(d\)](#).

[Insert Fig. 3]

In regard to the thermal distribution in the concrete, it was found that the increased horn height in Fig. 5 produced a temperature of  $\frac{\lambda}{4}, \frac{\lambda}{2}, \frac{4\lambda}{4}, \lambda$  at 71.45, 72.33, 62.50, and 75.55°C, respectively. When the horn height is increased by  $\lambda$  to achieve a height of 273 mm, as presented in Fig. 5(d), the thermal distribution in the surface of the concrete improves, i.e., becomes more even. In addition, the thermal distribution widens and hot and cold spots are reduced, as presented in Fig. 3.

[Insert Fig. 3]

[Insert Fig. 4]

[Insert Fig. 5]

It is emphasized that the height adjustment of the horn produces an electric field of  $8.74e^4 \times 10^4$  V/m, as presented in Fig. 4(d), and a thermal distribution at 75.55°C. After this height optimization, the horn width is adjusted by the steps described next.

For simulation Case 2, the electric fields are  $1.134e^5 \times 10^5$  V/m and  $9.06e^4 \times 10^4$  V/m when the horn width is increased, as presented in Figs. 6(a) and 6(b), respectively. IN Fig. 6(a), it is shown that the increased horn width produces better electric distribution in terms of the electric field. In addition, the distribution of the concrete temperature found at 79.45°C is presented in Fig. 6(c) and that found at 78.99°C, in Fig. 6(d). Therefore, if the horn width is increased, as presented in Fig. 6(a), the electric field in the horn will increase. This electric

field increase, in turn, facilitates the process whereby the material or load can receive the electric field, which can produce the concrete thermal distribution and increase the thermal distribution at the surface.

[Insert Fig. 6]

For Case 3, the electric fields of the reduced-width horn, as presented in Figs. 7(a) and 7(b), are  $9.835e^4 \times 10^4$  V/m and  $9.981e^4 \times 10^4$  V/m, respectively. It was found that if the horn width is reduced, the size of the electric field decreases. The thermal distribution within the concrete load is 72.04 and 70.61, as presented in Figs. 7(c) and 7(d), respectively.

[Insert Fig. 7]

With the horn design based on the concept of an antenna, the electric distribution within the horn is  $1.02e^5 \times 10^5$  V/m, as presented in Fig. 3(a), and the temperature of the load/concrete is 75.35°C. After increasing the horn height, increasing and reduction of horn found that the electric field is  $1.134e^5 \times 10^5$  V/m, as presented in Fig. 6(a), and the concrete temperature is 79.45°C. These results show that by increasing the distribution of electricity, or multimode wave and temperature.

## EXPERIMENTS

A concrete was mixed and poured into molds. Two kinds of cases were explored: conventional curing (air curing and water curing) and microwave curing (fixed mode and movement mode).

### Materials

All the materials used in this study were obtained locally. The cementitious material used in all the mixtures was Type 1 Portland cement (OPC), which complies with ASTM C 150.<sup>[24]</sup> The tap water used conforms to ASTM C 1602.<sup>[25]</sup> Further, the fine and coarse aggregates also obtained locally as river sand and crushed limestone rock, respectively, were in accordance with ASTM C 33.<sup>[26]</sup>

## Equipment

The microwave-dryer prototype for concrete curing is presented in Fig. 8. The applied frequency of the microwave is 2.45 GHz, which is created by the horn with a magnetron waveguide installed. The power is set at 800 W to produce microwave energy. A programmable logic controller (PLC) System is applied to control the movement and on-off mode. The length of the rail is 2.5 m, and a motor to control the driving, AC type, 90 W is installed. A chain is used for driving and use gear, 13 pieces that have a gear ratio of 1:5 and the motor drive speed is 0.

[Insert Fig. 8]

## Specimen preparation

The mixture is weighed, mixed, and poured into an acrylic mold that has a thickness of 10 mm, which is designed to protect the mixture from the reflection of the microwave. The dimensions of the mold are 150 × 150 × 15 mm, as stated in the English standard BS 1881: PART 3.<sup>[27]</sup> The concrete is mixed according to the ASTM C 192 standard.<sup>[28]</sup> The mixture is left to develop for an initial setting time of 30 min. Then, the mixture is cured by using microwave energy. Next, the frame is removed from the mold and the curing continues but

now in the air by wrapping the mixture in a sealed plastic bag and keeping it at a temperature of  $25 \pm 2.0$  C for 12 h. Finally, the compressive strength of the mixture is tested.

[Insert Table 2]

Similarly for curing in water and air, the mixture is poured into a steel mold and cured for  $23\frac{1}{2} \pm \frac{1}{2}$  h. Then, concrete samples of the mixture are cured in water for 8 h, 1 day, 3 days, 7 days, 14 days, and 28 days, respectively. For curing in air, the mixture is wrapped and sealed in a plastic bag and kept in a controlled room, where the temperature is maintained in the range of  $25 \pm 2.0$  °C and relative moisture is maintained in the range of  $60 \pm 3.0$ . It is cured to maintain the testing time for 8 h, 1, 3, 7, 14, and 28 days. Finally, the compressive strength of the concrete is tested.

### **Cases study of microwave curing**

In this study, concrete curing is tested via a conventional method and by microwave curing in both the fixed and movement modes. Non-continuous microwave curing is carried out in the preheating phase by using microwave **energy** until a fixed time. Then, the heating is paused and the concrete is reheated using microwave **power**. The condition of curing is presented in **Table 3**. The details of each experiment are as follows:

- Case A: Concrete curing in water and air

For concrete curing in water and air, the frame is removed from the mold when the mixture is at age  $23\frac{1}{2} \pm \frac{1}{2}$  h. For water curing, the testing times are 8 h, 1 day, 3 days, 7 days, and 28 days. For air curing, the concrete is wrapped and sealed in a plastic bag and kept in the controlled room where the temperature is held at  $25 \pm 2.0$ °C and where the relative

moisture is held at approximately  $60 \pm 3.0$ . The curing is carried out for 8 h, 1 day, 3 days, 7 days, 14 days, and 28 days. Finally, the compressive strength of the concrete is tested.

- Case B: Concrete curing by using continuous microwave power of 800 W

The concrete is cured by using continuous microwave power of 800 W and tested at 30, 60, 90, and 120 min.

- Case C: Concrete curing by using continuous microwave power of 400 W

The concrete is cured by using continuous microwave power of 400 W and tested at 30, 60, 90, and 120 min.

- Case D: Concrete curing by using non-continuous microwave power of 800 W

The concrete is cured by using non-continuous microwave power of 800 W and tested at 30, 60, 90, and 120 min (not include the pause time). The PLC system is used to control the on/off switch for the microwave power.

- Case E: Concrete curing by using non-continuous microwave power of 800 W

The concrete is cured by using non-continuous microwave power of 800 W and tested at 30, 60, 90, and 120 min (not including the pause time). The PLC system is used to control the on/off switch for the microwave power.

- Case F: Concrete curing by using continuous microwave power of 800 W  
(movement system)

The concrete is cured by using microwave power of 800 W, and the PLC system is used to control the on/off switch for the microwave power and the movement, as shown in Fig. 9. There are six samples, each of which is cured by microwave energy for 180 min.

[Insert Fig. 9]

[Insert Table 3]

## Testing methods

### *Moisture content measurement*

The moisture content is measure is based on the weight of the mixed cubic concrete to find the initial weight of concrete specimen. After that, a microwave curing concrete of each curing time is wrapped and sealed in a plastic bag and kept at a temperature in the range of  $25 \pm 2.0^\circ\text{C}$  for 12 h. Then, the concrete is weighed to determine the final weight, after which the compressive strength is tested. Further, the wet bulb in the concrete can be calculated by using the following equation:

$$A = \left( \frac{W_a - W_b}{W_a} \right) \times 100 \quad (11)$$

where  $A$  is the wet bulb (%),  $W_a$  is the initial weight of the concrete before curing (kg), and  $W_b$  is the final weight after curing (kg).

### *Temperature measurement*

The temperature measurement of the concrete can be divided into two aspects: the internal temperature measurement and the external temperature measurement. The process of measuring begins by using a thermocouple wire Type T connected to a data logger and spike in the middle of the concrete. Three levels of concrete, the top, middle, and bottom, are all measured at 30, 60, 90, and 120 min.

The measurement is carried out at 1 cm from the top surface (top), 7.5 cm from the top surface (middle), and 14 cm from the top surface (bottom), as presented in [Fig. 10](#). The natural heat advection is assumed at the top surface because the wall side is insulated by the 10 mm thick acrylic. In addition, heat transpiration occurs only at the top surface and not at

the sides. The internal temperature is measured in order to establish the effect of the microwave-curing temperature for Cases B, C, D, and F.

### ***Compressive strength test***

Compressive strength—the maximum stress concrete can bear before cracking—is the most important property of concrete. The respective processes for testing the compressive strength of concrete by air and water curing and by microwave curing are carried out by following the standard set out in BS 1881:PART4.<sup>[29]</sup>

[Insert Fig. 10]

## **RESULTS AND DISCUSSION**

In this section, the results of the tests focused on the thermal behavior of concrete during microwave curing, the thermal distribution on the concrete surface, the residual moisture content after microwave curing, and the compressive strength of the concrete are discussed.

### **Thermal behavior of concrete under microwave curing (Case B)**

Fig. 11 presents the effects of microwave curing of concrete with a 0.48 water–cement ratio under a 120 min curing time and 800 W electrical power (Case B). It is found that the temperature of the concrete increased continuously. At the beginning of the experiment, the moisture content of the concrete was high, which means that the transfer rate of microwave energy to heat takes place rapidly in accord with heat production theory.<sup>[17]</sup> After 90 min, the temperature is constant because the moisture content at the surface of the concrete is reduced due to the absorption capacity of the microwave energy. It can be



explained that the dielectric property of concrete is related to the reduced moisture whereas the internal structure of the concrete's voids means that excess water is retained (i.e., the free or residual water remaining after the chemical reaction). After being activated by the microwave energy, the concrete is absorbed and transmits heat energy. At the beginning of the curing process, the moisture content in the concrete has a direct effect on the initial temperature because the concrete's dielectric property is high. This causes the concrete's temperature to increase rapidly and continuously. However, as the moisture content in the concrete decreases, the dielectric property also decreases, rendering the concrete's temperature constant.

At the beginning of the curing process, the temperature at the top of the concrete increases continuously whereas the temperature in the middle intermittently increases. It can be explained that the top surface contains excess water and that bleeding occurs after curing for 30 min to develop initial setting time. At this stage, the concrete surface absorbs the microwave energy to a significant extent after 70 min of curing. However, the temperature in the middle increases rapidly because the temperature of 100°C at the top surface is high enough to transfer down as far as the middle. In addition, heat accumulates in the middle of the concrete and heat cannot occur because of the insulation wall. At the bottom, the temperature increases slowly due to the heat accumulation and the insulation wall. However, at 95 min, the heat increases dramatically from 70°C to 100°C. The temperature at the top surface is 110°C, and at the middle it is 103°C. Therefore, the heat transfer is conducted throughout the concrete sample. Then, at 100 min, the temperature throughout the concrete increases to 100°C. In addition, at 120 min, the temperature at the top surface is 125°C, at the middle it is 110°C, and at the bottom it is 100°C.

**[Insert Fig. 11]**

## **Influence of microwave power on the temperature of concrete under microwave curing**

### **(Case C)**

**Fig. 12** presents the results from the microwave curing of concrete at 400 W. The results show that the temperature of the concrete increased rapidly. The extent of the electrical power used is directly related to the temperature of the concrete. Low electrical power has a direct effect on the intensity of the electric field, which is a significant parameter of heat generation, as is well known.<sup>[30]</sup> In addition, a change in the amount of electric power used directly reduces directly the multi-mode within the horn. Curing the concrete for 30 min at 400 W can increase the concrete's temperature to 70°C, whereas curing by 800 W for 30 min can increase the concrete's temperature to 80°C. It was found that the behavior of heat generation within the concrete under both of these conditions is quite similar. At the beginning of the process, the temperature at the top surface is very high due to the high moisture content and the high dielectric property of the concrete, which microwave energy can absorb and transform entirely into heat energy. The temperature in the middle of the concrete increases continuously; penetrated microwave can increase the concrete temperature. Heat accumulates at the bottom of the concrete because of the insulation wall and the heat transferred from the surface. After 70 min, the temperature in the middle is changes rapidly due to a top surface temperature of 105°C. Then, the differing temperature in the middle and at the bottom is constant because 400 W is used to absorb the microwave energy of the dielectric material, which is related directly to the electric field. Therefore, heat generation in the concrete decreases. At the bottom, the temperature is constant at 100°C after 90 min, indicating that electric or microwave power influences the heat generation of concrete due to changes in the electric field.

**[Insert Fig. 12]**

### **Thermal behavior of concrete under discontinuous concrete curing (Case D)**

In this experiment, the concrete is tested in both the fixed mode and the movement mode at 800 W (Case B). The results show that the concrete's compressive strength decreases continuously after a curing time of 90 min and again after 120 min. When the concrete's temperature is higher than 80°C, <sup>[31]</sup> compressive strength decreases by 50%. By observation, at a curing time of 120 min, it was found that the temperature at the top, middle, and bottom of the concrete are 125, 115, and 100°C, respectively. These results may have a negative effect on the internal structure of the concrete, which may crack thus giving rise to low compressive strength. Therefore, discontinuous microwave curing is applied in order to maintain the appropriate temperature, which can increase the compressive strength of concrete. This experiment was carried out by using the PLC system to control the microwave supply or on/off mode, as presented in Fig. 13.

[Insert Fig. 13]

Fig. 13 presents the discontinuous curing by microwave energy (Case D). The experiment is carried out by preheating for 20 min, idle time for 2 h, energized by microwave power for 10 min and idle time for 2 h until the total time is 2 h. The total time of this experiment is 22 h, and the total microwave curing time is 120 min. The results show that in the first 20 min, the temperature at the top, in the middle, and at the bottom of the concrete is approximately 68, 50, and 43°C, respectively. After that, the PLC serves the function of stopping the microwave supply for 2 h and reheating for 10 min. This working loop is operated for 120 min (including only the energizing time and excluding the idle time). During the idle time, the temperature at the top, in the middle, and at the bottom is reduced to 20, 10, and 5°C, respectively. These phenomena can be explained by noting that the top surface is

exposed to air because of heat advection, such that the temperature decreases. The temperature in the middle decreases slowly and at the bottom the temperature decreases slightly as there is no heat advection.

### **Heat evolution from discontinuous curing (Case E)**

**Fig. 14** presents the discontinuous curing by microwave energy (Case E). In this experiment, the moisture content still retained in concrete and compressive strength is increased slightly. Therefore, the energizing time of microwave has been added and idle time has been reduced to achieve high temperature and remove moisture. The experiment is carried out by microwave energizing for 30 min, idle time for 1 h and re-energize for 15 min and second idle time for 1 hour until the total time reaches 120 min. The total time is 8 h, and the curing time is 120 min, which is controlled by the on/off system of the PLC. In the first 30 min, the temperature of the top, middle, and bottom part are 81, 55, and 41°C, respectively. The operating loop composes of 1-hour idle time and 15 minute energizing microwave. The results expressed that temperature is increased continuously due to energizing time is increased and idle time is reduced. The temperature at the top, middle, and bottom 110, 83, and 65°C, respectively. In addition, the moisture content and the compressive strength of the concrete are both higher than these respective properties under discontinuous curing (Case D).

**[Insert Fig. 14]**

### **Thermal distribution at the concrete surface**

The internal temperature of the concrete after the application of microwave curing is carried out by measuring the temperature in various parts of the samples. The absorption

phenomenon whereby microwave energy is transformed into heat energy while the temperature increases continuously is shown in Fig. 15. The external temperature at the top surfaces and sides of the samples is recorded by using an infrared camera. The results indicate that heat in the concrete wall is evident at a depth of 3 to 5 cm depth from the top surface. After that, heat is dispersed to the top surface and the wall of the concrete, as shown in Fig. 16.

The heat distribution at the concrete surface differs in accord to whether 800 W and 400 W of microwave power are applied. The electrical power has a direct effect on the intensity of the electric field. In addition, the temperature increases as the curing increases. The maximum temperature in the concrete occurred at 3 to 5 cm from the top surface.

[Insert Fig. 15]

[Insert Fig. 16]

## **Drying Characteristics of a Porous Concrete Material Subjected to Microwave Energy**

### ***Moisture loss***

In this experiment, a water–cement ratio is equal to 0.48 for all the studied cases. For the purpose of repairing concrete roads, the highway department sets a maximum limit on the water and cement (w/c) of 0.55 by weight. The water or moisture content in concrete means that concrete is a dielectric material capable of absorbing microwave energy and transforming it into heat. Therefore, when concrete is energized by microwave power, the moisture content of the concrete or the excess water from hydration between the cement and water is reduced. In addition, the concrete is energized by continuous microwave power, the moisture content

decreases and thereby affects the moisture-transfer mechanism in the concrete (porous material theory).

The results pertaining to the amount of moisture lost from the concrete after microwave curing in Cases B, C, D, and E are presented in Fig. 17. Overall, the moisture content of the concrete undergoes rapid changes at the beginning of the curing phase. The moisture distribution is related to many factors, i.e., the porosity of the concrete, moisture content transfer from within the concrete to its surface, the changing state from liquid to gas phase, and the moisture transfer from the thermal distribution. At first, the moisture content at the surface of the concrete absorbs microwave energy, which is then transformed into heat energy. The rate of evaporation is equal to the water movement in porous materials that creates the liquid film. The controlled parameter is the level of the heat energy input into the concrete. When the process whereby moisture is removed has been carried out, the internal moisture is reduced (as presented in Figure 3.7: the porous material theory), and this reduced moisture content has a direct effect on the concrete's dielectric property. The moisture content is reduced, and the heat generation is reduced likewise (heat transfer and mass in porous material).

[Insert Fig. 17]

### ***Compressive strength development***

Compressive strength is the most important property of concrete. The main function of concrete is load resistance, which is a direct function of compressive strength. Further, compressive strength is an indicator of other important properties, namely, durability, friction resistance, and porosity resistance.

This research focuses on concrete with compressive strength of at least  $325 \text{ kg/cm}^2$  for concrete at age 28 days. Microwave technology is applied in order to accelerate the curing time because a road repair carried out based on conventional curing can mean that a road is out of use for as many as 14 days. For this special case, compressive strength must be not less than  $245 \text{ kg/cm}^2$ .

The experiment whereby concrete is curing using microwave energy is divided into two parts: the conventional case (Case A), air and water curing, and microwave curing for Cases B, C, D, and E and moving curing (Case F).

**Fig. 18** presents water and air curing (Case A). The results indicate that the concrete's compressive strength increased rapidly in the first 3 days. The initial curing phase can increase this property of concrete. During the first 3 days, water curing and air curing show a similar level of efficiency. After that period, however, under water curing, the concrete's compressive strength increases continuously until the age of 28 days when the compressive strength is equal to  $405.59 \text{ kg/m}^2$ . On the other hand, under air curing after the first 3 days, the concrete shows only a slight increase in compressive strength until the age of 28 days when the compressive strength is equal to  $332.17 \text{ kg/cm}^2$ . The results show that water curing yields a higher level of compressive strength than air curing does. This is because under water curing, the moisture content facilitates the chemical reaction between cement and water, which serves to develop this concrete property.

**[Insert Fig. 18]**

**[Insert Fig. 19]**

Fig. 19 presents results pertaining to continuous microwave curing and discontinuous microwave curing for Cases B, C, D, and E. The results show that the compressive strength of the concrete as cured in Case B is increased continuously at 30 and 60 min. Then, after 90 and 120 min, the compressive strength decreased continuously. Temperature has an effect on compressive strength development. In Case C, the curing at 400 W, the electrical power can continuously increase the compressive strength. However, the compressive strength of the concrete in Case C increased slightly in comparison with the compressive strength of the concrete in Case B.

For Cases D and E, microwave energizing was changed to a discontinuous mode and these two cases show the same level of compressive strength. The preheating together with the reduced idle-time and reduced energized time are important factors in developing the concrete strength in Case D.

Fig. 20 presents the compressive strength of microwave curing in the movement mode (Case F). The curing time is 18 h, 180 min of microwave curing (not including idle time). The results indicate that the compressive strength levels of all six samples are similar. The average compressive strength is  $193.45 \text{ kg/cm}^2$ . The speed of motor for the movement study is 5 rpm with discontinuous microwave energy applied. The PLC is applied in order to control horn movement.

The discontinuous microwave curing used in Case E produces a high level of compressive strength when compared with the compressive strength developed in the respective Case C, and Case D samples. Therefore, more experiments were performed. The curing time was extended by 60 min. Thus, the total time during which microwave energy is applied for Case E is 180 min. The total time of this experiment is 13 h for microwave curing.

The results show that compressive strength increases to  $239 \text{ kg/cm}^2$  whereas moisture content after curing decreased to 53.3%. It can be concluded that this increased curing time



can increase the compressive strength of the concrete and reduce its moisture content.

However, the internal temperature is 113°C, which should be studied in the future in order to determine the appropriate curing time and mixture design given the direct effects of water in concrete on the thermal distribution.

[Insert Fig. 20]

## CONCLUSION

In this research, microwave-drying technology is applied to accelerated concrete curing. From the design and construction of a microwave-dryer prototype and an experimental investigation into compressive strength of concrete dried using the prototype, the following conclusions can be drawn:

- The scope of the prototype design has many factors, i.e., the 1-axis movement and horn must be adjusted in a vertical direction [up-down], at 800 W power, and 2.45 GHz frequency.
- The effect microwave energy transformed into heat on concrete material activated is studied in regard to temperature, moisture content, and curing time.
- The appropriate preheating interval is 30 min and microwave energizing for 15 min/time and a paused duration of 60 min produces maximum compressive strength.
- The highest strength achieved by microwave curing is 239 kg/cm<sup>2</sup>, which is equal to 85% of the strength achieved by water curing. Thus, discontinuous microwave curing for 120 min represents a reduction in curing time as compared with the time needed for water curing, for 3 days and 7 days.

## ACKNOWLEDGEMENTS

The authors gratefully acknowledge the Thailand Research Fund under the TRF contract Nos. RTA5680007 and TRG5780255, and the National Research Universities Project of the Higher Education Commission for supporting this research. Also, the authors acknowledge Mr. Poncharoen Chanamai for his assistance in collecting laboratory data.

## REFERENCES

1. Regier, M.; Schubert, H. Microwave processing. In *The Microwave Processing of Foods*, Schubert, H and Regier, M., Eds; Woodhead Publishing, Sawston: Cambridge, USA, 2001.
2. Afrin, N.; Zhang, Y.; Chen, J.K. Thermal lagging in living biological tissue based on non-equilibrium heat transfer between tissue, arterial and venous bloods. *International Journal of Heat and Mass Transfer* 2011, 54, 2419–2426.
3. Perre, P.; Turner, I. W. Microwave drying of softwood in an oversized waveguide: Theory and experiment, *AIChE Journal* 1997, 43(10), 2579–2595.
4. Choi, Y.; Okos, M.R. Thermal properties of liquid foods review. In: Okos, M.R. (Ed.), *Physical and Chemical Properties of Food*. American Society of Agricultural Engineers, St. Joseph, MI, 1986, 5–77.
5. Chang, K.; Ruan, R. R.; Chen, P. L. Simultaneous heat and moisture transfer in cheddar cheese during cooling. I. Numerical simulation. *Drying Technology* 1998, 16(7), 1447–1458.
6. Kaensup, W.; Wongwises, S.; Chutima, S. Drying of pepper seeds using a combined microwave fluidized bed dryer. *Drying Technology* 1998, 16(3–5), 853–862.
7. Basak, T., Role of resonance on microwave heating of oil–water emulsions. *AIChE Journal* 2004a, 50, 2659–2675.

8. Mujumdar, A.S., Handbook of Industrial Drying: 4<sup>th</sup> ed – CRC Press, Boca Raton, Florida, USA, 2014.
9. Leung, K.Y.; Pheeraphan, T. Microwave curing of Portland cement concrete: Experimental results and feasibility for practical applications. *Construction and Building Materials* 1995, 67–73.
10. Rattanadecho, P.; Suwannapuma, N., Chatveera, B., At-ong, D., Makul, N. Development of compressive strength of cement past under accelerated curing by using a continuous microwave thermal processor *Material Science and Engineering* 2008, A 472, pp. 299–307.
11. Makul, N.; Rattanadecho, P.; Agrawal, D.K. Microwave curing at operating frequency of 2.45 GHz of Portland cement paste at early-stage using a multi-mode cavity: Experimental and numerical analysis on heat transfer characteristics. *International Journal of Heat and Mass Transfer* 2010, 37, 1487–1495.
12. American Concrete Institute. ACI 318–Building Code Requirements for Structural Concrete and Commentary. Farmington Hills, MI, 2008.
13. Watson, A. Curing of Concrete, *Microwave Power Engineering* 1968, 2, 108 –118.
14. Xuequan, W. Microwave curing technique in concrete manufacture. *Cement and Concrete Research*, 1987, 17(2), 205–210.
15. Hutchison, R.G. Thermal acceleration of Portland cement mortars with microwave energy. *Cement and Concrete Research*, 1991, 21(5), 795–799.
16. Sohn, D.; Johnson, D.L. Microwave Curing Effect on the 28 day Strength of Cementitious Materials. *Cement and Concrete Research*, 1999, 29, 241–247.
17. Metaxas, A.C.; Meredith, R.J. *Industrial Microwave Heating*, Peter Peregrinus, Ltd., London, 1983.

18. Jeppson, M.R.; Calif, C. Microwave Method and Apparatus for Heating Pavement. United States Patent, 4252487, 1981.
19. Hopkins, H.C. Microwave Highway Paint Drying Apparatus. United States Patent, 4765773, 1988.
20. Figg, J. Microwave Heating in Concrete Analysis. *Journal of Applied Chemistry and Biotechnology* 1974, 24(3), 143–155.
21. Sipherd, C.B.; Lease, J.R.; Stainbrook, R.L. Concrete Curing Machine. United States Patent, 6497531 B1, 2002.
22. COMSOL Multiphysics User's Guide Version 3.4, COMSOL AB, Singapore, 2007.
23. Campanone, L.A.; Zaritzky, N.E. Mathematical Analysis of Microwave Heating Process. *Journal of food Engineering* 2005, 69, 359–368.
24. American Society for Testing and Materials. ASTM C150 – 12 Standard Specification for Portland Cement. *Annual Book of ASTM Standard Vol. 4.01*, Philadelphia, PA, USA., 2012.
25. American Society for Testing and Materials. ASTM C1602 / C1602M - 12 Standard Specification for Mixing Water Used in the Production of Hydraulic Cement Concrete. *Annual Book of ASTM Standard Vol. 4.02*, Philadelphia, PA, USA, 2012.
26. American Society for Testing and Materials. ASTM C33 / C33M - 13 Standard Specification for Concrete Aggregates. *Annual Book of ASTM Standard Vol. 4.02*, Philadelphia, PA, USA, 2013.
27. British Standards Institution. BS 1881: PART 3, Method of making and curing test Specimen. London, United Kingdom, 2011.
28. American Society for Testing and Materials. ASTM C192 / C192M - 14 Standard Practice for Making and Curing Concrete Test Specimens in the Laboratory. *Annual Book of ASTM Standard Vol. 4, No. 02*, Philadelphia, PA, USA., 2014.

29. British Standards Institution. BS 1881:PART 4: Method of testing concrete for strength. London, United Kingdom, 2011.
30. Rattanadecho, P.; Aoki, K.; Akahori, M. Experimental and numerical study of microwave drying in unsaturated porous material. *International Journal of Heat and Mass Transfer* 2001a, 28, 605–616.
31. Sohn, D.; Johnson, D.L. Microwave curing effect on the 28 day strength of Cementitious materials. *Cement and Concrete Research* 1999, 29, 241–247.

## FIGURES

**FIG. 1** Horn design process.

**FIG. 2** Physical model for distribution analysis of the magnetic field in the cavity and thermal distribution in the concrete.

**FIG. 3** (a) Distribution of magnetic field within the horn (without load case) from the first result of the horn design. (b) Thermal distribution (with load case) integrated with the first horn design.

**FIG. 4** (a) Height of original horn of  $\frac{\lambda}{4}$  is equal to 181.2 mm. (b) Height of original horn of  $\frac{\lambda}{2}$  is equal to 211.8 mm. (c) Height of original horn of  $3\frac{\lambda}{4}$  is equal to 242.4 mm. (d) Height of original horn of  $\lambda$  is equal to 273 mm.

**FIG. 5** (a) Thermal distribution for height  $\frac{\lambda}{4}$  is equal to 181.2 mm. (b) Thermal distribution for height  $\frac{\lambda}{2}$  is equal to 211.8 mm. (c) Thermal distribution for height  $3\frac{\lambda}{4}$  is equal to 242.4 mm. (d) Thermal distribution for height  $\lambda$  is equal to 273 mm.

**FIG. 6** (a) Adjustment of horn of 246.7 mm × 333.68 mm. (b) Adjustment of horn of 256.7 mm × 347.2 mm. (c) Adjustment of horn of 246.7 mm × 333.68 mm and thermal distribution. (d) Adjustment of horn of 256.7 mm × 347.2 mm and thermal distribution.

**FIG. 7** (a) Reduction of horn size of 226.7 mm × 306.64 mm. (b) Reduction of horn size of 216.7 mm × 293.12 mm. (c) Adjustment of horn size of 246.7 mm × 333.68 mm and thermal distribution. (d) Reduction of horn size of 216.7 mm × 293.12 mm.

**FIG. 8** (a) Horn configurations constructed as a prototype. (b) Prototype for microwave curing

**FIG. 9** Flow diagram of process for microwave-curing of concrete (movement system).

**FIG. 10** Installation of a thermocouple to measure the internal temperature of concrete.

**FIG. 11** Temperature profile of concrete with continuous microwave curing (Case B).

**FIG. 12** Internal temperature of concrete after continuous curing by microwave energy (Case C).

**FIG. 13** Temperature of concrete under discontinuous curing.

**FIG. 14** The internal temperature of concrete after curing by discontinuous microwave curing (Case E).

**FIG. 15** (a) Heat distribution after microwave curing of Case B for (a) 30 min, (b) 60 min, (c) 90 min, and (d) 120 min.

**FIG. 16** (a) heat distribution after microwave curing of Case C for (a) 30 min, (b) 60 min, (c) 90 min, and (d) 120 min.

**FIG. 17** Moisture content in concrete.

**FIG. 18** Compressive strength of concrete after water and air curing (Case A).

**FIG. 19** Compressive strength of concrete after microwave curing.

**FIG. 20** The compressive strength of microwave curing in the moving mode (Case F).

**TABLES****TABLE 1**

Input data for analysis

Symbol	Value	Unit
$\epsilon_0$	$8.85419 \times 10^{-12}$	<i>F/m</i>
$\mu_0$	$4\pi \times 10^{-7}$	<i>H/m</i>
$\epsilon_r$	10	–
<i>t</i>	60	<i>s</i>
$c_p$	650	<i>J/kg.k</i>
$\rho$	2300	<i>Kg/m<sup>3</sup></i>
Power	800	<i>W</i>
<i>f</i>	2.45	<i>GHz</i>
$T(t_0)$	298.15	<i>k</i>
<i>k</i>	0.87	<i>w/m.k</i>

**TABLE 2**

Mixture ratio of concrete (per 1 cubic meter of concrete)

Type 1 Portland Cement (kg)	Water (kg)	River sand (kg)	Crushed limestone rock (kg)	Water–cement ratio (by mass)
350	170	830	1135	0.48

**TABLE 3**

Conditions for curing

Case	Power (W)	Preheating (min)	Pause (min)	Heating (min)	Total (min)
Case A	Air, Water	–	-	–	8 h, and 1, 3, 7, 14, 28 days
Case B	800	Continuity	–	–	30, 60, 90, 120
Case C	400	Continuity	–	–	30, 60, 90, 120
Case D	800	20	120	10	30, 60, 90, 120
Case E	800	30	60	15	30, 60, 90, 120
Case F	800	30	60	10	30, 60, 90, 120



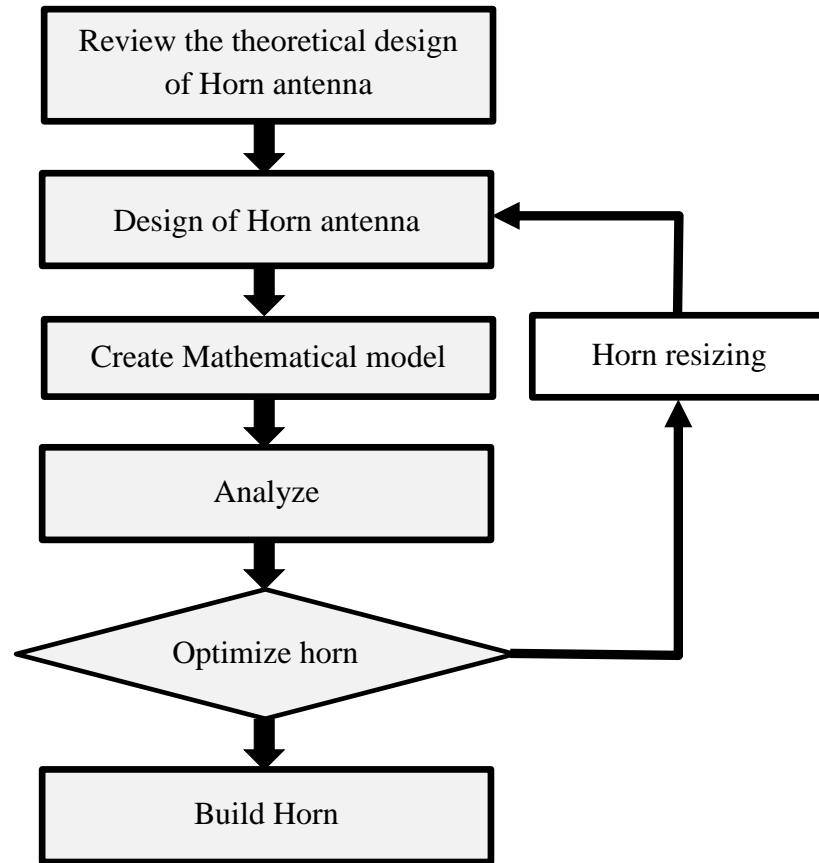


**FIG. 1** Horn design process.

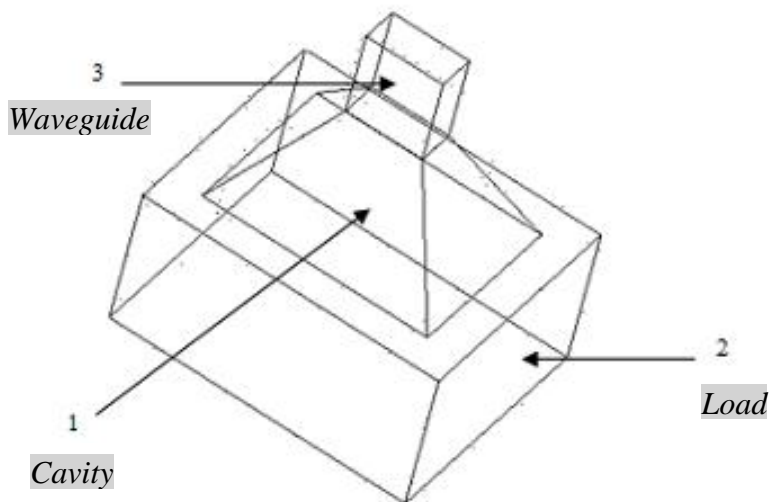


**FIG. 2** Physical model for distribution analysis of the magnetic field in the cavity and thermal distribution in the concrete.

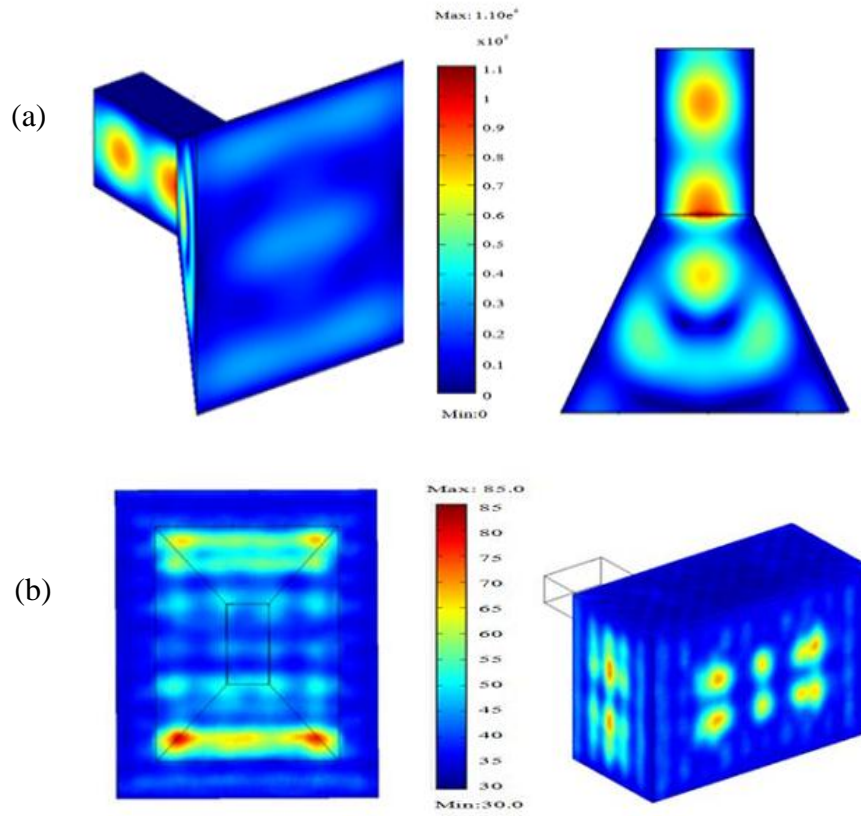


**FIG. 3** (a) Distribution of magnetic field within the horn (without load case) from the first result of the horn design. (b) Thermal distribution (with load case) integrated with the first horn design.

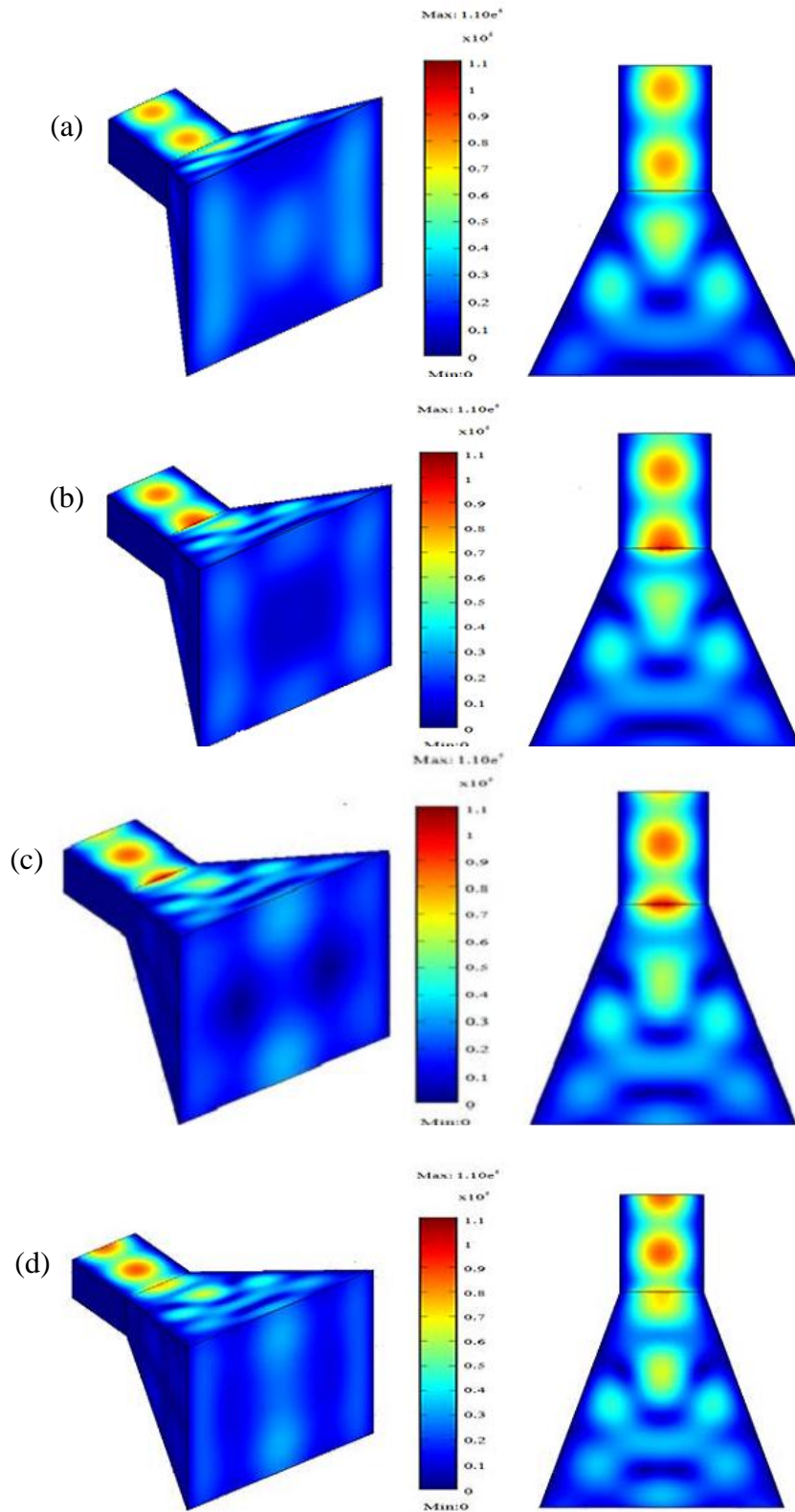


**FIG. 4** (a) Height of original horn of  $\frac{\lambda}{4}$  is equal to 181.2 mm. (b) Height of original horn of  $\frac{\lambda}{2}$  is equal to 211.8 mm. (c) Height of original horn of  $3\frac{\lambda}{4}$  is equal to 242.4 mm. (d) Height of original horn of  $\lambda$  is equal to 273 mm.

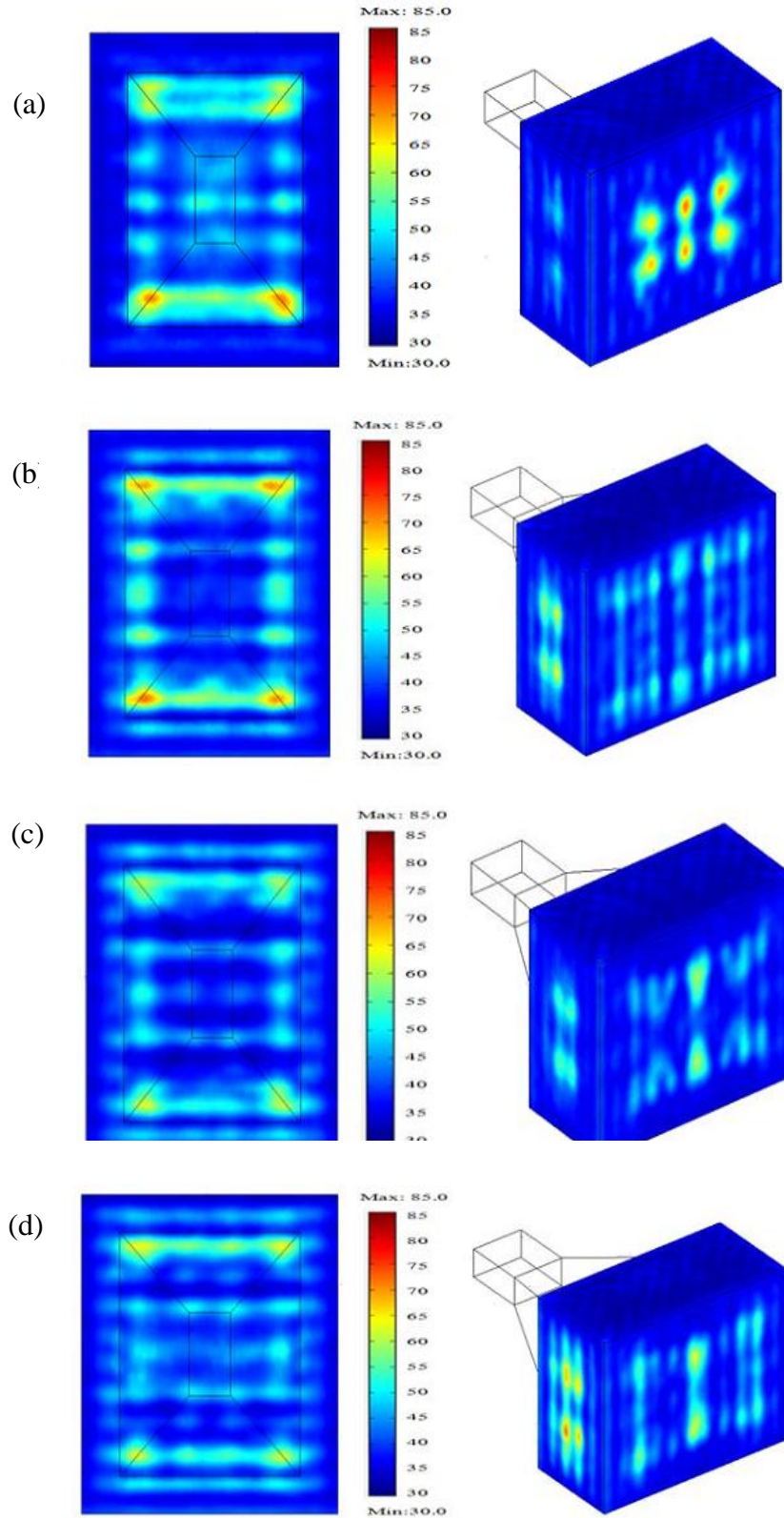


**FIG. 5** (a) Thermal distribution for height  $\frac{\lambda}{4}$  is equal to 181.2 mm. (b) Thermal distribution for height  $\frac{\lambda}{2}$  is equal to 211.8 mm. (c) Thermal distribution for height  $3\frac{\lambda}{4}$  is equal to 242.4 mm. (d) Thermal distribution for height  $\lambda$  is equal to 273 mm.

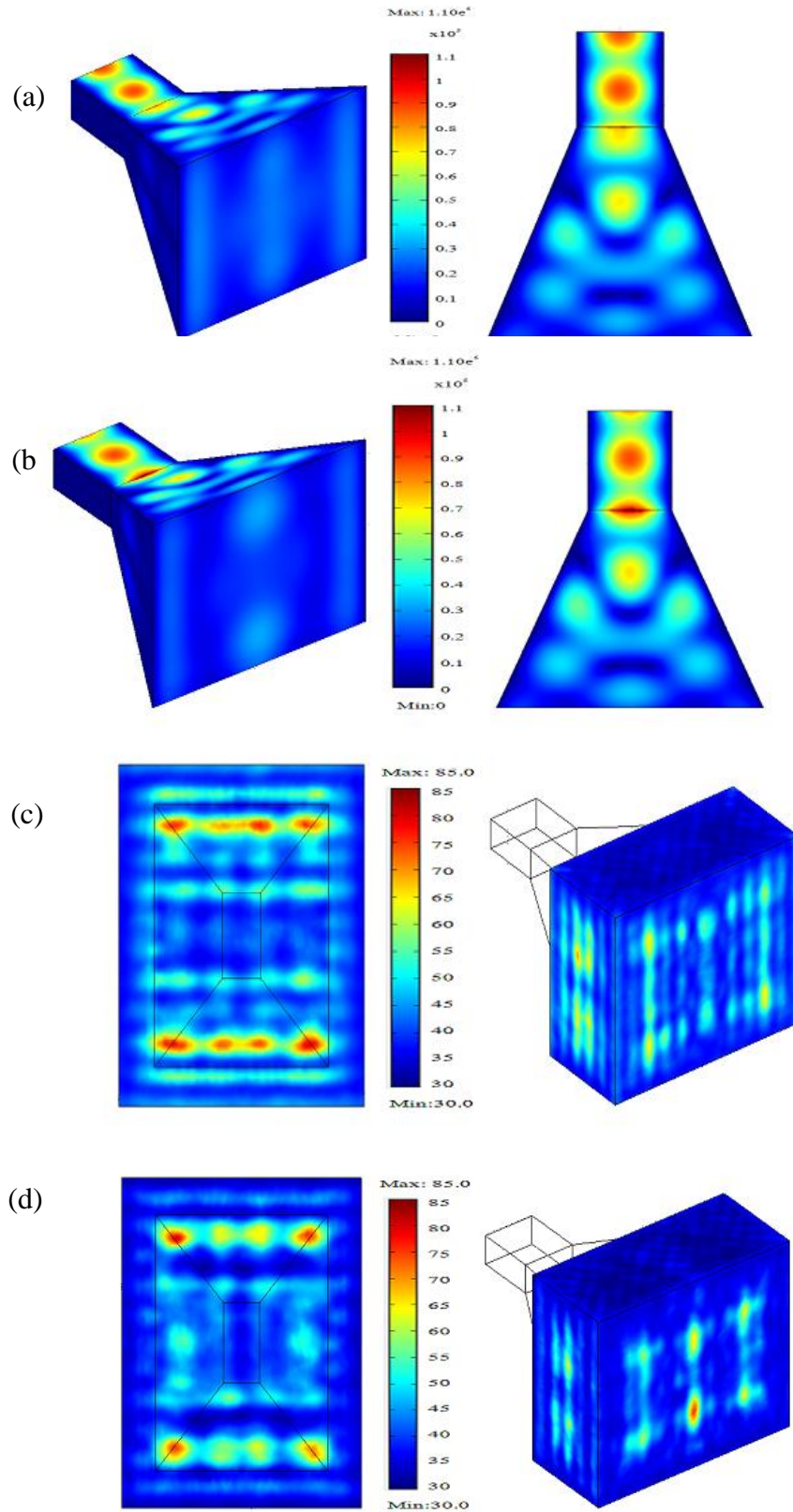


**FIG. 6** (a) Adjustment of horn of 246.7 mm × 333.68 mm. (b) Adjustment of horn of 256.7 mm × 347.2 mm. (c) Adjustment of horn of 246.7 mm × 333.68 mm and thermal distribution. (d) Adjustment of horn of 256.7 mm × 347.2 mm and thermal distribution.

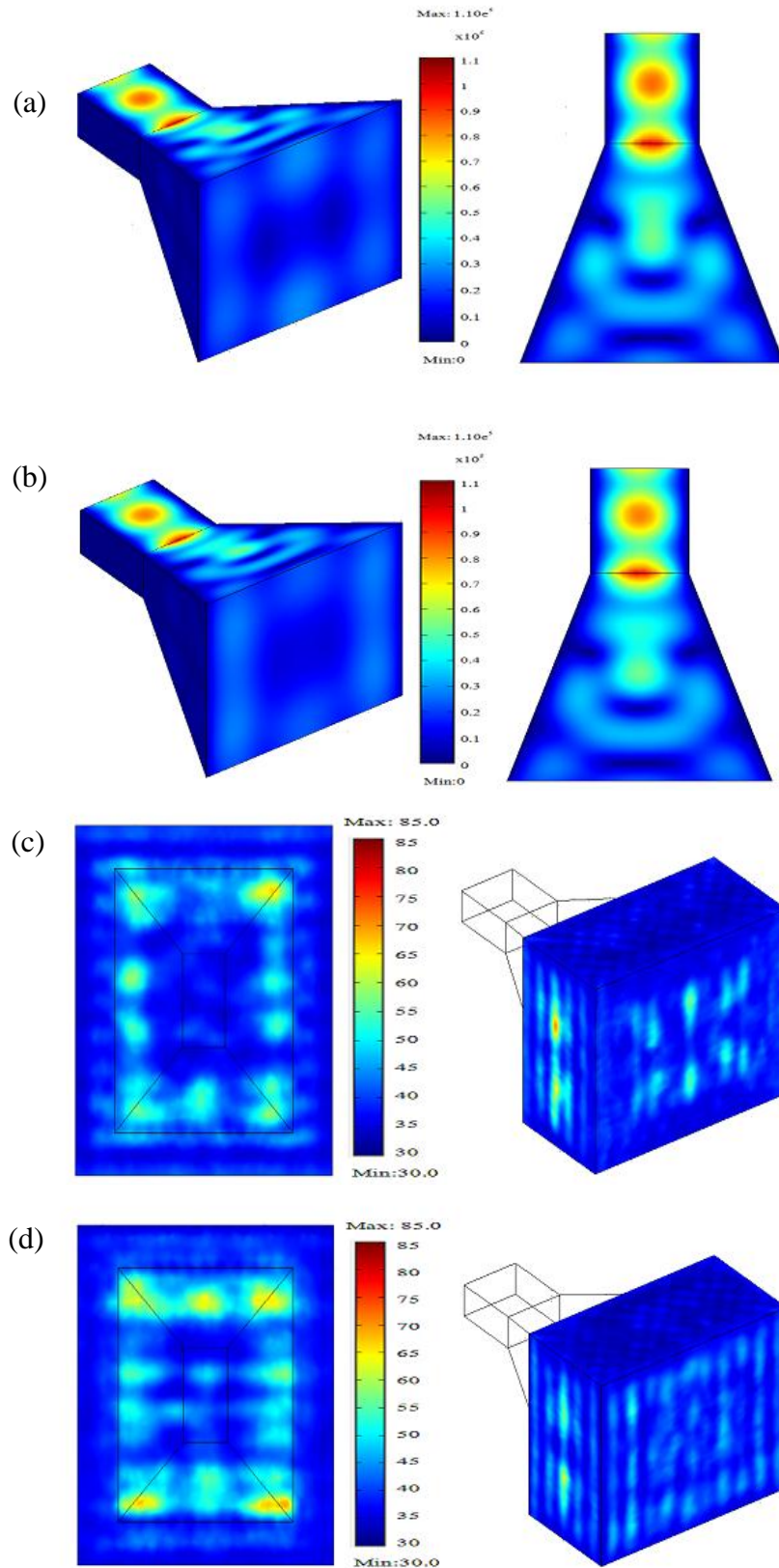


**FIG. 7** (a) Reduction of horn size of 226.7 mm × 306.64 mm. (b) Reduction of horn size of 216.7 mm × 293.12 mm. (c) Adjustment of horn size of 246.7 mm × 333.68 mm and thermal distribution. (d) Reduction of horn size of 216.7 mm × 293.12 mm.

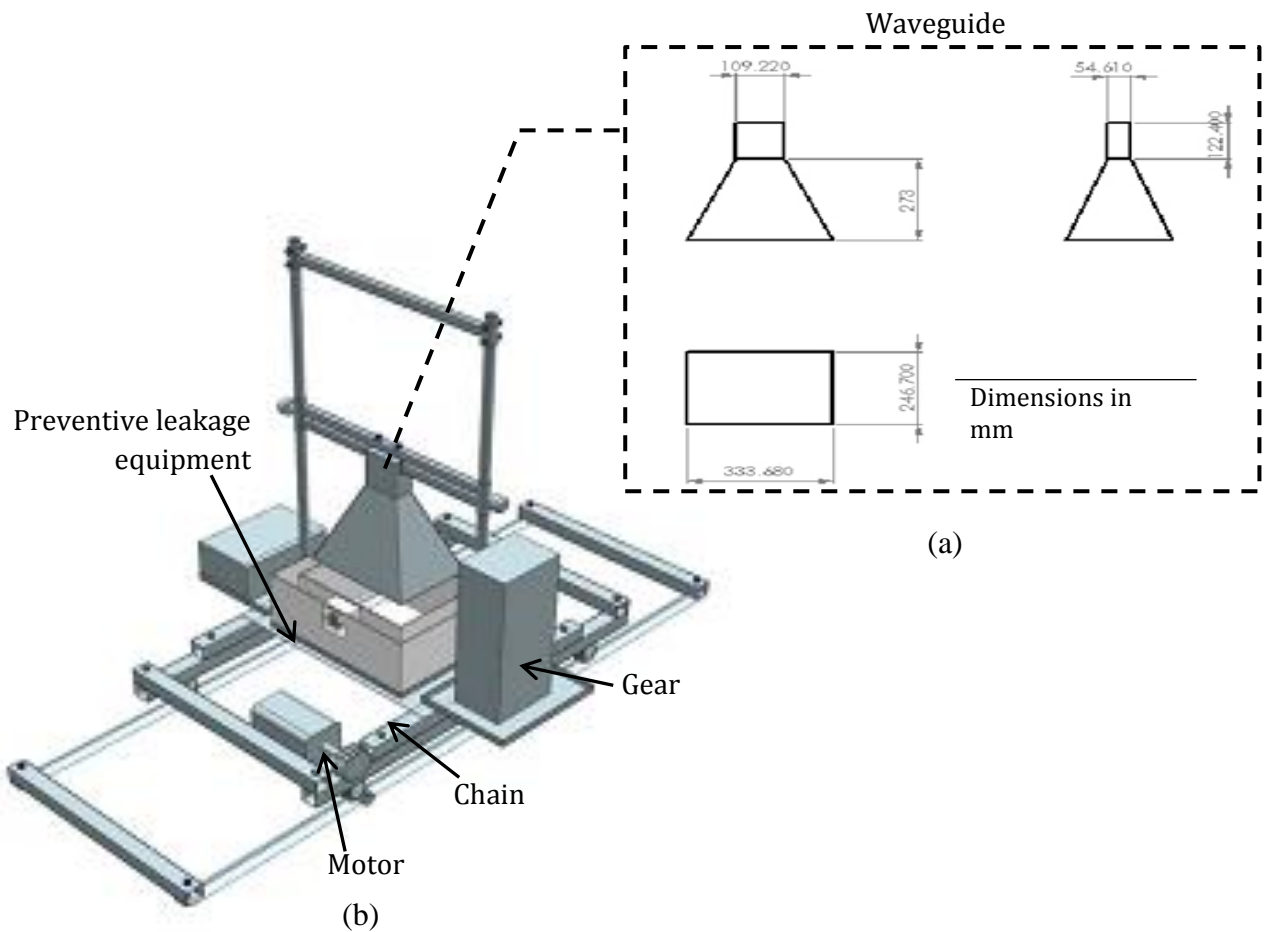


**FIG. 8** (a) Horn configurations constructed as a prototype. (b) Prototype for microwave curing.

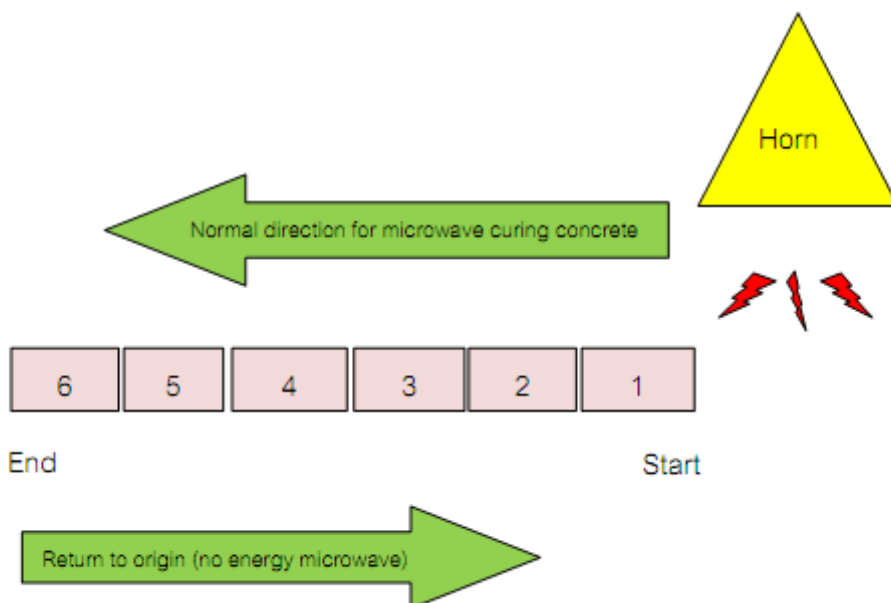


**FIG. 9** Flow diagram of process for microwave-curing of concrete (movement system).

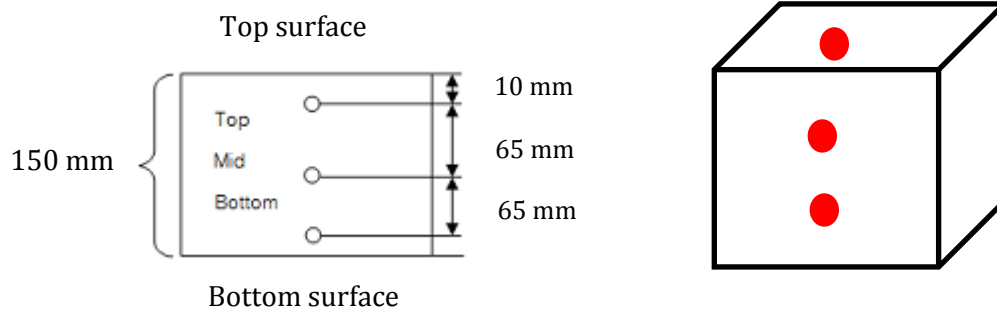


**FIG. 10** Installation of a thermocouple to measure the internal temperature of concrete.

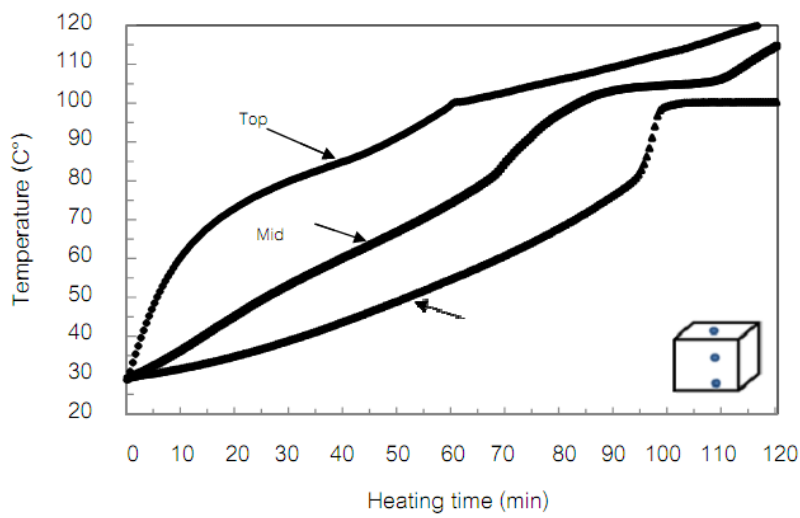


**FIG. 11** Temperature profile of concrete with continuous microwave curing (Case B).

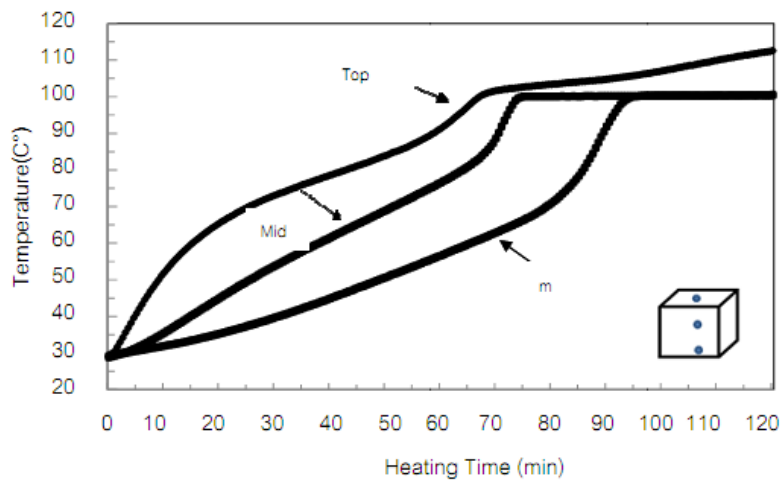


**FIG. 12** Internal temperature of concrete after continuous curing by microwave energy (Case C).



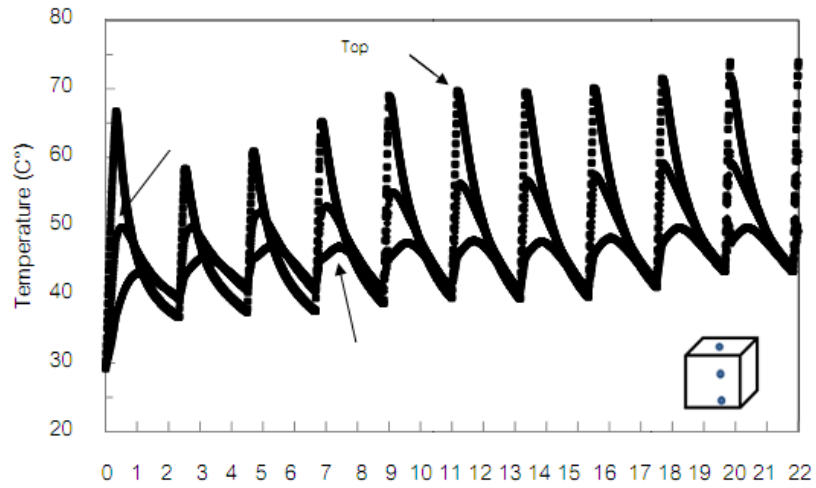


**FIG. 13** Temperature of concrete under discontinuous curing.

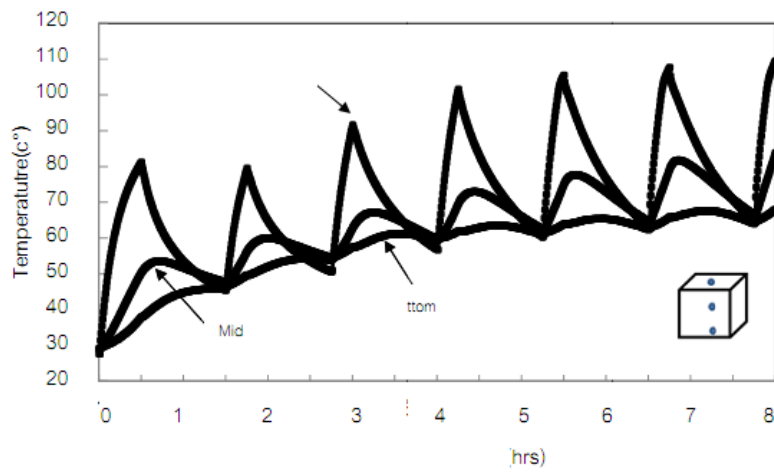


**FIG. 14** The internal temperature of concrete after curing by discontinuous microwave curing (Case E).

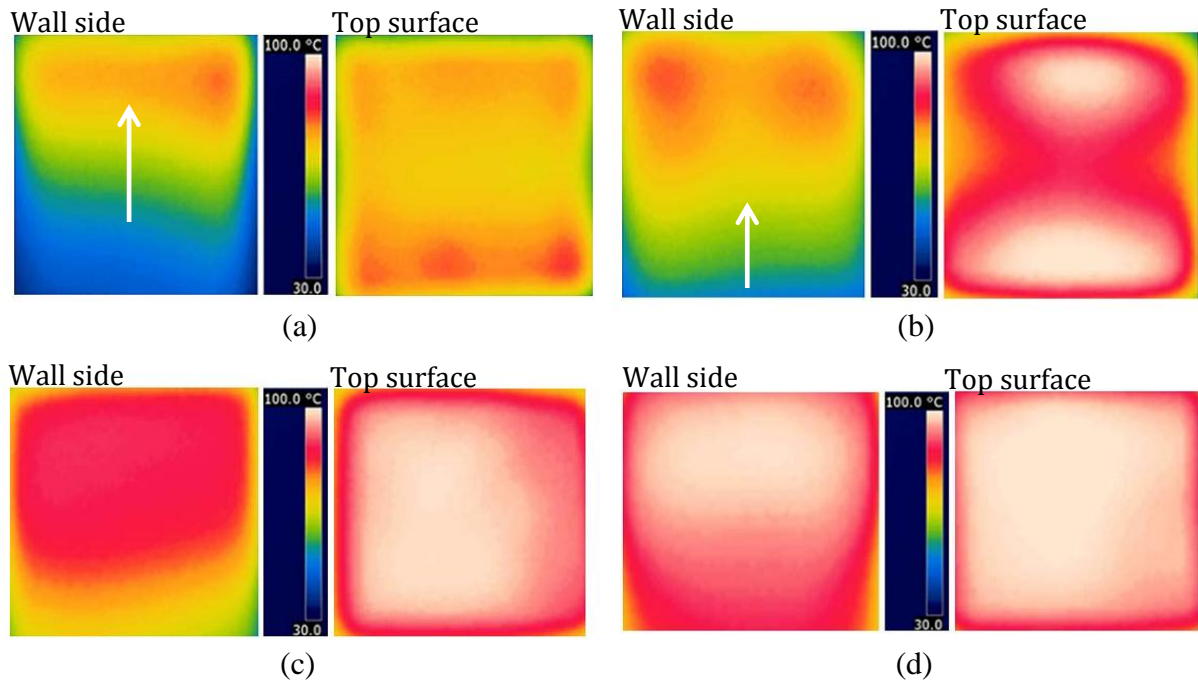


**FIG. 15** (a) Heat distribution after microwave curing of Case B for (a) 30 min, (b) 60 min, (c) 90 min, and (d) 120 min.

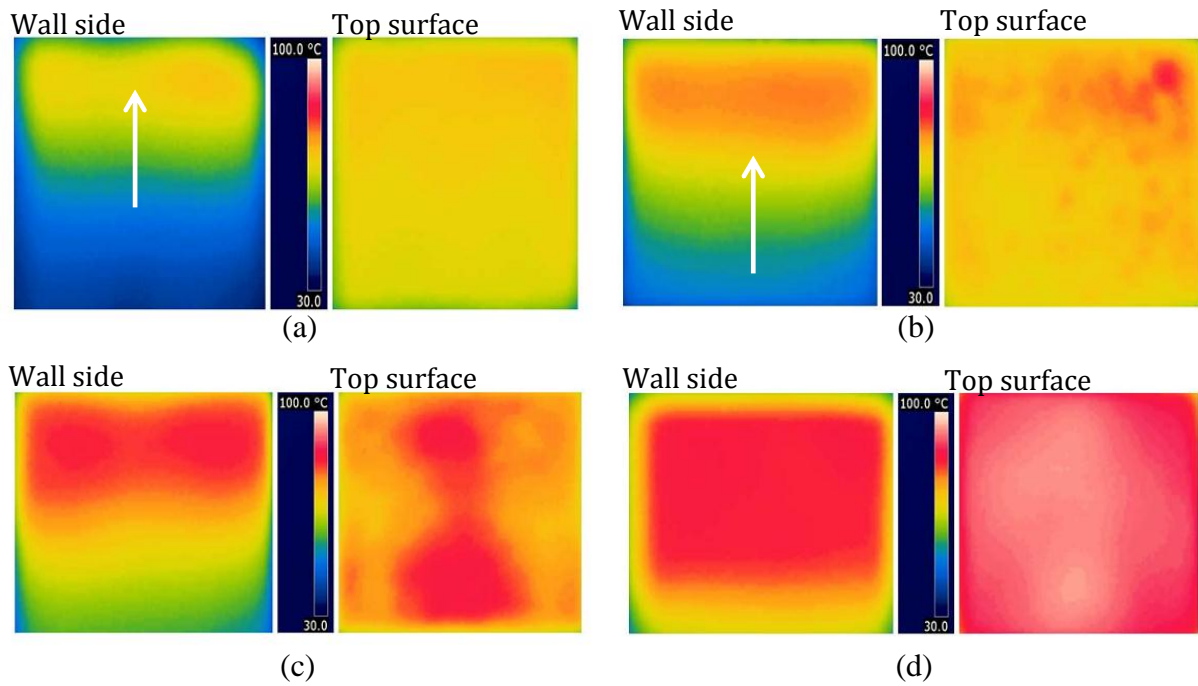


**FIG. 16** (a) heat distribution after microwave curing of Case C for (a) 30 min, (b) 60 min, (c) 90 min, and (d) 120 min.

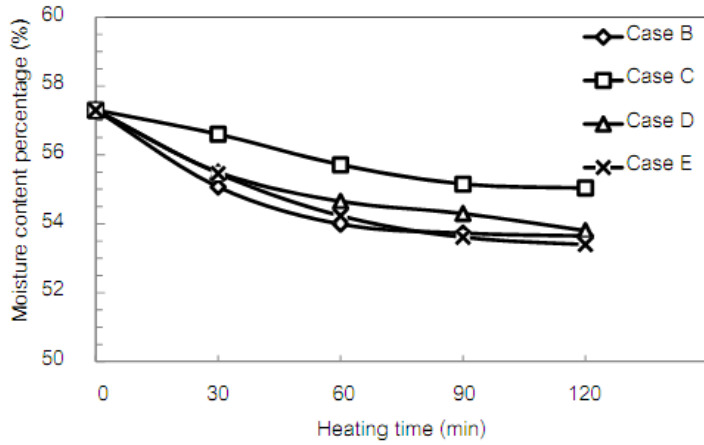


FIG. 17 Moisture content in concrete.

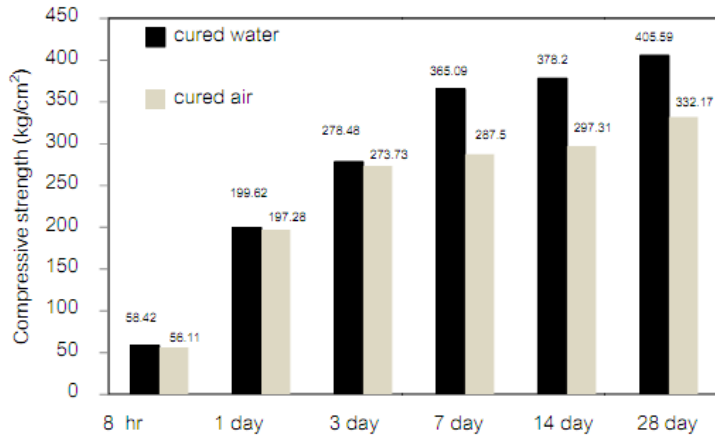


FIG. 18 Compressive strength of concrete after water and air curing (Case A).

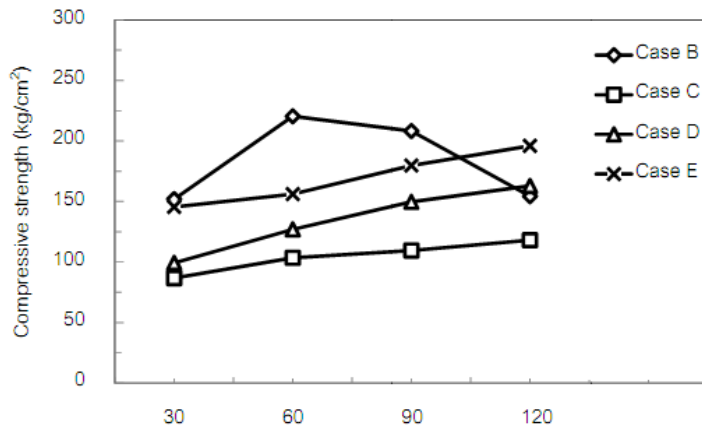
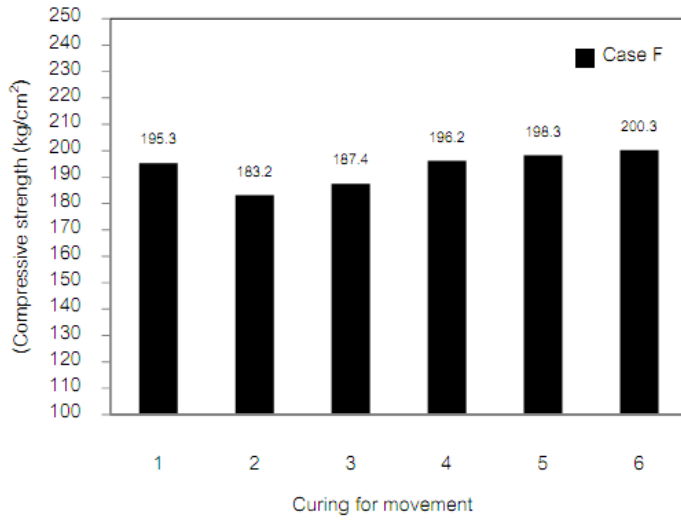


FIG. 19 Compressive strength of concrete after microwave curing.



**FIG. 20** The compressive strength of microwave curing in the moving mode (Case F).